NANO EXPRESS

Optical properties and bandgap evolution of ALD HfSiO$_x$ films

Wen Yang[1], Michael Fronk[2], Yang Geng[1], Lin Chen[1*], Qing-Qing Sun[1*], Ovidiu D Gordan[2], Peng zhou[1], Dietrich RT Zahn[2] and David Wei Zhang[1]

Abstract

Hafnium silicate films with pure HfO$_2$ and SiO$_2$ samples as references were fabricated by atomic layer deposition (ALD) in this work. The optical properties of the films as a function of the film composition were measured by vacuum ultraviolet (VUV) ellipsometer in the energy range of 0.6 to 8.5 eV, and they were investigated systematically based on the Gaussian dispersion model. Experimental results show that optical constants and bandgap of the hafnium silicate films can be tuned by the film composition, and a nonlinear change behavior of bandgap with SiO$_2$ fraction was observed. This phenomenon mainly originates from the intermixture of d-state electrons in HfO$_2$ and Si-O antibonding states in SiO$_2$.

Keywords: HfSiO$_x$; VUV; Bandgap

Background

With the downscaling of CMOS devices, high-k materials are required to replace SiO$_2$ as gate dielectrics in order to decrease the direct tunneling leakage current and, at the same time, maintain the gate capacitance at a certain value [1-7]. Among the potential candidates, hafnium silicate was chosen as the first generation of high-k dielectrics for its high dielectric constant and excellent thermal stability [8,9]. Compared to other deposition methods used for hafnium silicate film fabrication, atomic layer deposition (ALD) has the advantages of precise film thickness and stoichiometry control, which are of great significance to optimize the material especially for the shrinking devices [10-15].

Since accurate determination of the optical properties is an essential prerequisite for device simulations and gives the opportunity to improve material preparation, we have applied vacuum ultraviolet (VUV) spectroscopic ellipsometry to investigate the optical characteristics of a set of hafnium silicate films in this work. It will also gain us an insight into the effect of film composition on the electrical performance and chemical states of hafnium silicate dielectric films.

Methods

The targeted HfSiO$_x$ thin films were deposited on lightly doped p-type Si (100) substrates by a BENEQ TFS-200 ALD system (BENEQ Oy, Espoo, Finland) at 200°C. The Si wafers were cleaned via RCA cleaning process at first, then prior to film growth, they were cleaned again in a diluted HF solution (50:1) to remove the native oxide and passivate the silicon dangling bonds followed by a de-ionized water rinsing and drying in N$_2$. During deposition process, precursors for Hf, Si, and O were TEMAH, TDMAS, and O$_2$ plasma respectively. TEMAH was kept at 80°C in a stainless bottle, and TDMAS was kept at room temperature. The O$_2$ plasma was activated at the power of 100 W. Typical pulsing sequences during the ALD process are 1/3/2/2 s (TEMAH/Ar purge/O$_2$ plasma/ Ar purge) and 2/2/2/2 s (TDMAS/Ar purge/O$_2$ plasma/Ar purge) for the growth of HfO$_2$ and SiO$_2$ films, respectively. For the HfSiO$_x$ films, SiO$_2$ percentage was controlled by deposition cycle ration of HfO$_2$: SiO$_2$. Pure HfO$_2$, SiO$_2$, and five groups of HfSiO$_x$ samples with different atomic compositions were prepared.

For optical characterization, each sample was measured using a Woollam variable-angle vacuum ultraviolet spectroscopic ellipsometer (SE), and the data were analyzed with the software Complete EASE by J.A. Woollam. The measurements were taken at two angles of incidence, 67.5° and 75°, with a spectroscopic range of 0.6 to 8.5 eV.

* Correspondence: linchen@fudan.edu.cn; qqsun@fudan.edu.cn
[1]Institute of Advanced Nanodevices, School of Microelectronics, Fudan University, No. 220 Handan Road, Shanghai 200433, China
Full list of author information is available at the end of the article

Yang *et al. Nanoscale Research Letters* (2015) 10:32

Page 2 of 5

Then, to determine the optical properties of the target samples, such as layer thickness and optical constants, the model-based analysis were carried out. Complete EASE includes a wide range of built-in functions, such as Lorentz, Gaussian, Drude, Tauc-Lorentz, and Cody-Lorentz. These functions can be used to approach a wide variety of thin film, ranging from dielectrics and organics to semiconductors and metals. In this work, the Cauchy dispersion relation was adopted for the determination of the films thickness and the optical properties were analyzed with the Gaussian dispersion model.

Results and discussion

The low energy range of each spectrum (0.6 to 4 eV) was used to determine the thickness of the sample by Cauchy dispersion relation, which is often adopted to describe the refractive index for transparent films in the visible spectral range. The Cauchy formula can be given by $n(\lambda) = A + \frac{B}{\lambda^2} + \frac{C}{\lambda^4}$. The extinction coefficient k equals 0 at all used wavelengths. In this equation, the 'A' parameter relates to the approximate amplitude for the material index, while 'B' and 'C' parameters provide the shape and curvature of the index versus wavelength. Film thicknesses of each sample obtained from Cauchy dispersion relation are listed in Table 1 (in the table HfSiO$_x$ films are denoted as $(HfO_2)_{1-x}(SiO_2)_x$, where x refers to different Si concentrations) together with the MSE values. 'MSE' is an acronym for mean squared error. It is the metric used to quantify the agreement between the experimental data and the parameterized optical model. 'Perfect' agreement would yield a MSE value equal to 0, and large deviations away from 0 will lead to erroneous extracted physical values (i.e., thickness and optical constants) [16,17]. From Table 1, it can be seen that for all samples, MSEs are very small values, and error bar of each sample is at least 2 magnitudes smaller than the thickness obtained, proving the correctness of extracted thickness.

To analyze the optical properties (behavior of refractive index and extinction coefficient), film thickness acquired

Table 1 Thickness of samples by Cauchy dispersion relation

	Thickness (nm)	MSE
HfO$_2$	9.80 ± 0.015	0.613
(HfO$_2$)$_{0.95}$(SiO$_2$)$_{0.05}$	12.00 ± 0.020	0.983
(HfO$_2$)$_{0.8}$(SiO$_2$)$_{0.2}$	10.39 ± 0.021	0.810
(HfO$_2$)$_{0.6}$(SiO$_2$)$_{0.4}$	9.36 ± 0.026	1.035
(HfO$_2$)$_{0.4}$(SiO$_2$)$_{0.6}$	8.80 ± 0.026	1.019
(HfO$_2$)$_{0.2}$(SiO$_2$)$_{0.8}$	11.36 ± 0.039	0.661
SiO$_2$	11.13 ± 0.049	0.641

MSE = mean squared error.

above were fixed and Gaussian dispersion model was used with the fitted range expanded to 0.6 to 8.5 eV. The Gaussian oscillator features a Gaussian line shape for the imaginary part of the complex dielectric function ε_2, with a Kramers-Kronig consistent line shape for the real part of the dielectric function ε_1 [18]:

$$\varepsilon_{n2} = A_n e^{-((E-E_n)/B_{rn})} + A_n e^{-((E+E_n)/B_{rn})} \quad (1)$$

$$\varepsilon_{n1} = \varepsilon_1(\infty) + \frac{2}{\pi} P \int_{E_g}^{\infty} \frac{\zeta \varepsilon_{n2}(\zeta) d\zeta}{\zeta^2 - E^2} \quad (2)$$

In the equations above, the P stands for the Cauchy principal part of the integral. The Gaussian oscillator model employs four setting parameters: the amplitude A, the broadening parameter B_r, the center energy E_n, and the non-dispersive term $\varepsilon_1(\infty)$. The two fitting parameters B_r and E_n are in units of energy while A and $\varepsilon_1(\infty)$ are dimensionless. $\varepsilon_1(\infty)$ represents the contribution of the optical transitions at higher energies and appears as an additional fitting parameter [19].

As an example, the experimental SE data Ψ and Δ of HfSiO$_x$ sample with 80% SiO$_2$ are shown in Figure 1. For both incidence angles, fairly good agreement between the experimental and fitted spectra are clearly demonstrated, revealing that the Gaussian model works well and optical constants of the film can be exactly determined by the best fitting results. Data of other samples are not shown here due to space limitations, but fitted data for all samples match as well with the experimental data.

Figure 2a shows the refractive index n as a function of photon energy for all samples as deduced from the analysis of the SE results. The n value for HfO$_2$ measured at 550-nm (2.26 eV) wavelength is 1.84, which is similar with the previous report [20]. In addition, as shown in
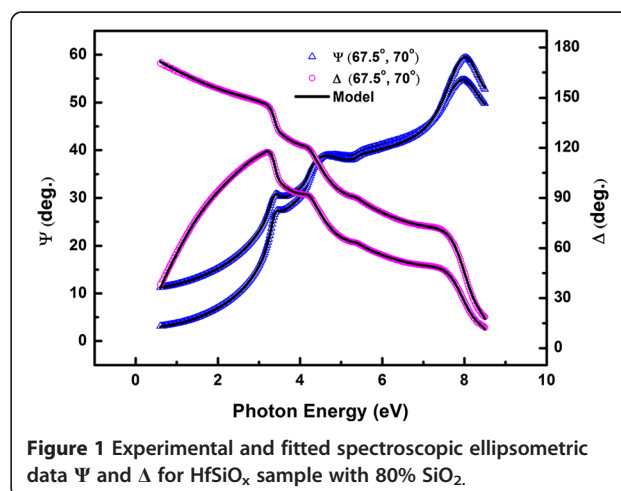

Figure 1 Experimental and fitted spectroscopic ellipsometric data Ψ and Δ for HfSiO$_x$ sample with 80% SiO$_2$.

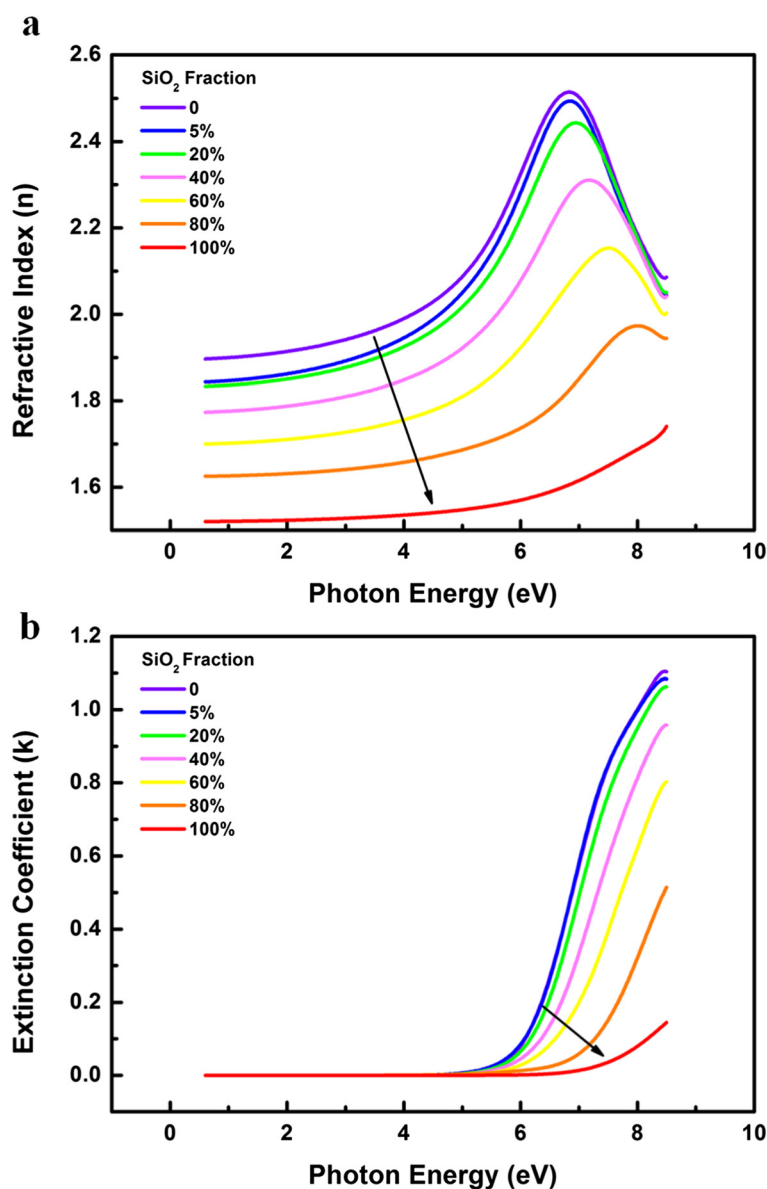Yang *et al. Nanoscale Research Letters* (2015) 10:32

Page 3 of 5

Figure 2 Calculated *n* (a) and *k* (b) of the HfSiO$_x$ films with different SiO$_2$ incorporation content.

Figure 2a, the index of refraction decreases with the increase of Si concentration in the films. According to the Lorentz-Lorenz relation [21], the refractive index can be related to the evolution of packing density and polarization. Since Si-O bonds tend to be less polar than the corresponding Hf-O bond [22], the increase of Si concentration in the film would lead to a decrease of the film polarization, then lower polarizability results in the lowering of the refractive index.

The evolution of extinction coefficient *k* is shown in Figure 2b. For all samples, *k* saturates to zero in the visible region, suggesting the realization of high quality HfSiO$_x$ films in terms of optical properties. An abrupt

increase in the extinction coefficient for higher photon energy is due to the fundamental bandgap absorption in the films. Moreover, as can be seen in Figure 2b, there is also a mall band tail below the gap. This weak absorption is attributed to the Urbach tail which exists below the bandgap of amorphous materials and due to the disorder of the amorphous network [23,24]. Furthermore, with the increase of Si concentration, decrease in the magnitude of the exponential tail can be observed, and similar results were obtained by the Cody-Lorentz model and Tauc-Lorentz model [16]. According to J. Price et al., this phenomenon is attributed to Si atoms filling the O$_2$ vacancies/defects in the HfO$_2$ films. By filling

Yang et al. Nanoscale Research Letters (2015) 10:32

Page 4 of 5

these vacancies, there is less disorder and therefore, less intraband absorption.

Optical bandgap of the films were determined by plotting the empirical expression $(n\alpha h\nu)^{1/2}$ versus $h\nu$, as shown in Figure 3, where n, α, and $h\nu$ stand for the index of refraction, the absorption coefficient, and the photon energy, respectively. The absorption coefficient α can be easily obtained by the equation $\alpha = 4\pi k/\lambda$, where λ is the wavelength of the incidence light [25]. By extrapolating the straight near the band edge to zero, the crossing point with the x-axis is considered to be the optical bandgap of the film. To make it clear, bandgap determination of HfO_2 is taken as an example and is shown in the inset of Figure 3. The extracted bandgap of pure HfO_2 film is 5.64 eV, in good agreement with the previously reported values 5.25 to 5.8 eV for HfO_2 [23,26,27].

Based on the method depicted above, the set of optical bandgaps acquired in Figure 3 is plotted in Figure 4 for details. As an exception, the bandgap of pure SiO_2 is not shown in Figure 4, because although the fitted range is sufficient for most of the samples, it is not for pure SiO_2 and the linear part of the curve in Figure 3 has not appeared yet. It is clearly demonstrated in Figure 4 that with increasing Si concentration, there is a monotonically increase in the bandgap of the films. This change mainly originates from the slight difference in electronic structure. And if we go into details, it can be found that E_g increases rapidly when SiO_2 fraction is more than 60%. The similar nonlinear change of $HfSiO_x$ bandgap with Si concentration was also observed by others [28,29]. It is known that the nonbonding O $2p$ states form the top of the SiO_2 valence band and that the Si-O antibonding states form the bottom of its conduction band [17]. In the case of HfO_2, the top of valence band are also composed of O $2p$ states but the bottom of conduction band states are mostly composed of Hf
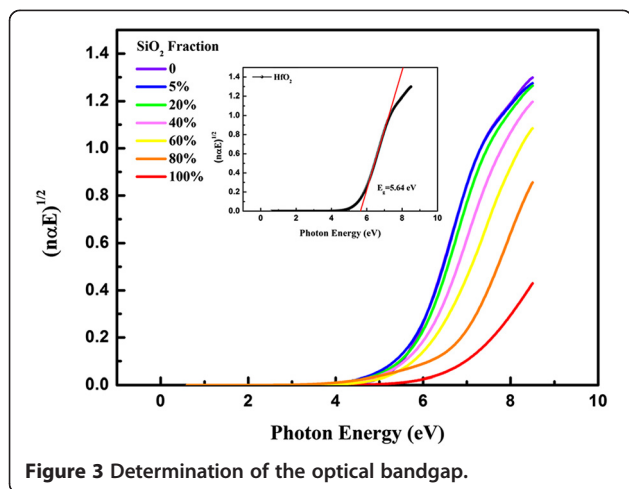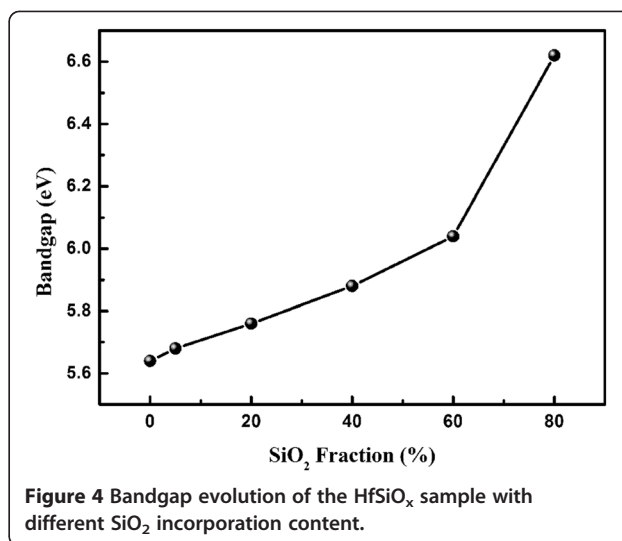

Figure 4 Bandgap evolution of the $HfSiO_x$ sample with different SiO_2 incorporation content.

localized $5d$ state [28]. Similar to the explanation given by H. Kato et al. in the case of $ZrSiO_x$ film [29], the rapid decrease in E_g with an increase in Hf concentration is considered to be attributed to the increase in the d-state electrons. When Si fraction is lower than 0.6, it seems that the bottom of the conduction band is almost formed by the Hf d-states, leading to the gradual decrease in E_g.

Conclusions

The optical properties of ALD hafnium silicate films, together with pure HfO_2 and SiO_2 films as references, were investigated systematically based on Gaussian dispersion model. According to the results, optical constants and bandgap of the hafnium silicate films can be tuned by the film composition, and a nonlinear change behavior of bandgap with SiO_2 fraction was observed. This phenomenon mainly originates from the intermixture of d-state electrons in HfO_2 and Si-O antibonding states in SiO_2.

Authors' contributions
WY made physical tests, analyzed the results, and drafted the manuscript. YG carried out the manufacture of samples. MF made the optical tests and supplied valuable discussion about the analysis. LC and Q-Q S conceived of the study and participated in its design and coordination. LC, Q-Q S, ODG, PZ, DRTZ, and DWZ participated in the design of the study and helped to draft the manuscript. All authors read and approved the final manuscript.

Figure 3 Determination of the optical bandgap.

Yang *et al. Nanoscale Research Letters* (2015) 10:32

Page 5 of 5

Author details
[1]Institute of Advanced Nanodevices, School of Microelectronics, Fudan University, No. 220 Handan Road, Shanghai 200433, China. [2]Semiconductor Physics, Technische Universität Chemnitz, Reichenhainer Straße 70, Chemnitz D-09107, Germany.

References
1. Kopani M, Mikula M, Pinčík E, Kobayashi H, Takahashi M. FT IR spectroscopy of silicon oxide and $HfSiO_x$ layer formation. Appl Surf Sci. 2014;312:117–9.
2. Bothe KM, von Hauff PA, Afshar A, Foroughi-Abari A, Cadien KC, Barlage DW. Electrical comparison of HfO_2 and ZrO_2 gate dielectrics on GaN. IEEE T Electron Dev. 2013;60:4119–24.
3. Hsu HW, Huang HS, Chen HW, Cheng CP, Lin KC, Chen SY, et al. Time dependent dielectric breakdown (TDDB) characteristics of metal-oxide-semiconductor capacitors with HfLaO and HfZrLaO ultra-thin gate dielectrics. Solid State Electron. 2012;77:2–6.
4. Oh J, Myoung J, Bae JS, Lim S. Etch behavior of ALD Al_2O_3 on HfSiO and HfSiON stacks in acidic and basic etchants. J Electrochem Soc. 2011;158:D217.
5. Cheng X, Qi Z, Zhang G, Chen Y, Li T, Pan G, et al. The interface reaction of high-k $La_2Hf_2O_7$/Si thin film grown by pulsed laser deposition. Appl Surf Sci. 2009;256:838–41.
6. Dimoulas A, Vellianitis G, Mavrou G, Apostolopoulos G, Travlos A, Wiemer C, et al. $La_2Hf_2O_7$ high-κ gate dielectric grown directly on Si(001) by molecular-beam epitaxy. Appl Phys Lett. 2004;85:3205–7.
7. Wilk GD, Wallace RM, Anthony JM. High-κ gate dielectrics: current status and materials properties considerations. J Appl Phys. 2001;89:5243–75.
8. Geng Y, Yang W, Zhu S, Zhang Y, Sun Q, Lu H, et al. Effect of ozone treatment on the optical and electrical properties of HfSiO thin films. Appl Phy A. 2014;116:259–63.
9. Lee S, Yun D, Rhee S, Yong K. Atomic layer deposition of hafnium silicate film for high mobility pentacene thin film transistor applications. J Mater Chem. 2009;19:6857–64.
10. Gu YZ, Lu HL, Geng Y, Ye ZY, Zhang Y, Sun QQ, et al. Optical and microstructural properties of ZnO/TiO_2 nanolaminates prepared by atomic layer deposition. Nanoscale Res Lett. 2013;8:107.
11. Zheng S, Sun QQ, Yang W, Zhou P, Lu HL, Zhang DW. Modulation in current density of metal/n-SiC contact by inserting Al_2O_3 interfacial layer. Nanoscale Res Lett. 2013;8:116.
12. Fang RC, Sun QQ, Zhou P, Yang W, Wang PF, Zhang DW. High-performance bilayer flexible resistive random access memory based on low-temperature thermal atomic layer deposition. Nanoscale Res Lett. 2013;8:92.
13. Zhou P, Ye L, Sun QQ, Wang PF, Jiang AQ, Ding SJ, et al. Effect of concurrent joule heat and charge trapping on RESET for NbAlO fabricated by atomic layer deposition. Nanoscale Res Lett. 2013;8:91.
14. Ding SJ, Chen HB, Cui XM, Chen S, Sun QQ, Zhou P, et al. Atomic layer deposition of high-density Pt nanodots on Al_2O_3 film using $(MeCp)Pt(Me)_3$ and O_2 precursors for nonvolatile memory applications. Nanoscale Res Lett. 2013;8:80.
15. Ye ZY, Lu HL, Geng Y, Gu YZ, Xie ZY, Zhang Y, et al. Structural, electrical, and optical properties of Ti-doped ZnO films fabricated by atomic layer deposition. Nanoscale Res Lett. 2013;8:108.
16. Price J, Hung PY, Rhoad T, Foran B, Diebold AC. Spectroscopic ellipsometry characterization of $Hf_xSi_yO_z$ films using the Cody-Lorentz parameterized model. Appl Phys Lett. 2004;85:1701–3.
17. Griscom DL. The electronic structure of SiO_2: a review of recent spectroscopic and theoretical advances. J Non-Cryst Solids. 1977;24:155–234.
18. Khoshman JM, Kordesch ME. Vacuum ultra-violet spectroscopic ellipsometry study of sputtered BeZnO thin films. Optik - Int J Light Electron Opt. 2011;122:2050–4.
19. von Blanckenhagen B, Tonova D, Ullmann J. Application of the Tauc-Lorentz formulation to the interband absorption of optical coating materials. Appl Opt. 2002;41:3137–41.
20. Jerman M, Qiao ZH, Mergel D. Refractive index of thin films of SiO_2, ZrO_2, and HfO_2 as a function of the films' mass density. Appl Opt. 2005;44:3006–12.
21. Mergel D, Buschendorf D, Eggert S, Grammes R, Samset B. Density and refractive index of TiO_2 films prepared by reactive evaporation. Thin Solid Films. 2000;371:218–24.
22. He G, Zhang LD, Meng GW, Li GH, Fei GT, Wang XJ, et al. Composition dependence of electronic structure and optical properties of $Hf_{1-x}Si_xO_y$ gate dielectrics. J Appl Phys. 2008;104:104116.
23. Nguyen NV, Davydov AV, Chandler-Horowitz D, Frank MM. Sub-bandgap defect states in polycrystalline hafnium oxide and their suppression by admixture of silicon. Appl Phys Lett. 2005;87:192903.
24. Ferlauto AS, Ferreira GM, Pearce JM, Wronski CR, Collins RW, Deng X, et al. Analytical model for the optical functions of amorphous semiconductors from the near-infrared to ultraviolet: Applications in thin film photovoltaics. J Appl Phys. 2002;92:2424–36.
25. Xu Y, Chen L, Sun Q, Gu J, Lu H, Wang P, et al. Electronic structure and optical properties of Nb doped Al_2O_3 on Si by atomic layer deposition. Solid State Commun. 2010;150:1690–2.
26. Lim S, Kriventsov S, Jackson TN, Haeni JH, Schlom DG, Balbashov AM, et al. Dielectric functions and optical bandgaps of high-K dielectrics for metal-oxide-semiconductor field-effect transistors by far ultraviolet spectroscopic ellipsometry. J Appl Phys. 2002;91:4500–5.
27. Afanas Ev VV, Stesmans A, Tsai W. Determination of interface energy band diagram between (100)Si and mixed Al–Hf oxides using internal electron photoemission. Appl Phys Lett. 2003;82:245–7.
28. Jin H, Oh SK, Kang HJ, Cho MH. Band gap and band offsets for ultrathin $(HfO_2)_x(SiO_2)_{1-x}$ dielectric films on Si (100). Appl Phys Lett. 2006;89:122901.
29. Kato H, Nango T, Miyagawa T, Katagiri T, Seol KS, Ohki Y. Plasma-enhanced chemical vapor deposition and characterization of high-permittivity hafnium and zirconium silicate films. J Appl Phys. 2002;92:1106–11.